ChemComm

COMMUNICATION

View Article Online
View Journal | View Issue

Cite this: *Chem. Commun.*, 2025, **61**, 10119

Received 30th April 2025,
Accepted 4th June 2025

DOI: 10.1039/d5cc02471d

rsc.li/chemcomm

Alkyne hydrazones for Raman scattering spectroscopy†

Daniil Sosnin and Ivan Aprahamian *

We explored alkyne-functionalized hydrazone photoswitches and enhanced their performance, achieving improved UV resolution, higher photostationary states, and tunable alkyne shifts (up to 34 cm^{-1}), establishing hydrazones as promising high-resolution Raman spectroscopy imaging probes.

Photoswitchable systems are an indispensable tool in the ongoing pursuit after light-responsive materials,[1] catalysts,[2] imaging probes,[3] and energy storage applications.[4] The development of novel switchable frameworks that can address end-goal related problems is crucial for advancing these applications. Among the various photoswitches[5] available in the literature hydrazone photoswitches[6] have proven particularly versatile because of their synthetic accessibility, tunability and bistability.[7] Our recent study[8] into the effect of 1,2,3-triazole ring connectivity (*i.e.*, the product of a "click" reaction between an alkyne and azide) on the photoswitching properties of hydrazones, has piqued our interest into the effect of the alkyne group in the precursors on these properties. We were also intrigued by the fact that such alkyne groups, which vibrate in the cellular silent region,[9] can be used in vibrational spectroscopy studies, such as Raman scattering spectroscopy.[10] This technique has recently gained attention as an alternative to fluorescence spectroscopy for biological systems because of its much narrower signal bandwidth,[11] enabling the creation of libraries of labels with minimal spectral overlap between the reporter molecules, enabling multiplexing.[12] As with regular microscopy, the resolution of Raman spectroscopy is limited by the Abbe diffraction limit.[13] Recently, photoswitchable Raman probes based on diarylethene have been used to circumvent this limitation resulting in significantly improved cell imaging resolution.[14] To enhance sensitivity and contrast in super resolution imaging, there is still room for improvement in such systems in terms of isomerization photostationary states (PSSs) and alkyne band shift upon photoisomerization, which was limited to 19 cm^{-1}. Henceforth, the structural diversity of alkyne-containing photoswitches needs to be expanded, to proliferate the use of such probes in high-resolution Raman scattering spectroscopy.[15]

Here, we report a systematic study of hydrazones **1–6** (Fig. 1) designed to explore the impact of alkyne groups on the hydrazone photoswitching performance. By varying the alkyne substitution at the rotor position, we modulated the electronic and vibrational properties of the system. Furthermore, incorporating the electron-withdrawing NO_2 group at the stator position significantly improved the UV band separation and PSS. These modifications resulted in alkyne-photoswitches having tunable alkyne band shifts of up to 34 cm^{-1} as a function of *E*/*Z* photoisomerization, demonstrating the viability of these hydrazones as Raman scattering spectroscopy probes.

The synthesis of the six alkyne-containing hydrazone photoswitches **1–6** proceeded in good (38–74%) yields (Schemes S1, S2 and Fig. S1–S16, ESI†). The final and critical step involved the condensation of the alkyne-containing rotor unit with the appropriate hydrazine derivative of the stator. The condensation reaction was performed at low temperatures to suppress a competing intramolecular cyclization pathway (Schemes S4 and Fig. S17, ESI†). The hydrazones were obtained as predominantly the *E*

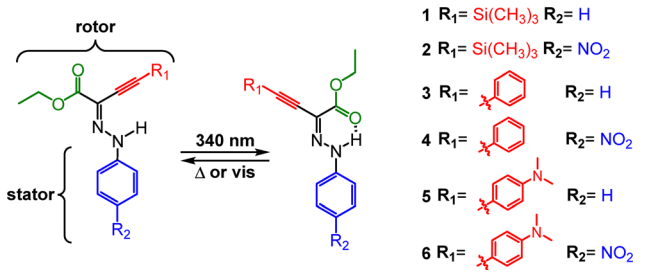

Fig. 1 The light-induced *Z*/*E* isomerization of the alkyne-containing hydrazone photoswitches **1–6** studied in this report. The stator and rotor designations are arbitrary and used to differentiate parts of the switch.

Department of Chemistry, Dartmouth College, Hanover, New Hampshire 03755, USA. E-mail: ivan.aprahamian@dartmouth.edu

† Electronic supplementary information (ESI) available. CCDC 2331026, 2331028, 2331030, 2331032, 2421979 and 2421980. For ESI and crystallographic data in CIF or other electronic format see DOI: https://doi.org/10.1039/d5cc02471d

isomer. This assignment was corroborated using the chemical shift of the NH proton, which resonates at 9 ppm in toluene-d_8, and X-ray crystallography analysis of the target molecules (Fig. S49, ESI†).

The photoswitching properties of hydrazones **1–6** were studied in toluene using UV/vis (Fig. S18–S23, ESI†), ^{1}H NMR, and Raman spectroscopies. We first focused on the simple trimethyl silyl (TMS) protected alkyne hydrazone **1**. The X-ray crystal analysis of **1** revealed that it is planar and adopts the E form (*i.e.*, there is no H-bond) (Fig. S49a, ESI†). The UV spectrum of **1**-*E* in toluene shows a maximum absorption (λ_{max}) at 359 nm (Fig. S18a, ESI†), representing a redshift compared to the parent phenyl hydrazone (λ_{max} = 334 nm).[15] Irradiating the sample with 340 nm light results in slight shift to a λ_{max} of 365 nm. The ^{1}H NMR spectrum shows that a PSS_{340} of 47% *Z* is obtained upon irradiation (Fig. S24b, ESI†), with an associated quantum yield (ϕ) of 8.4 ± 1.1% (Fig. S30, ESI†). Irradiation with 410 nm light results in the complete back isomerization to **1**-*E* (PSS_{410} 99%, $\Phi_{Z\rightarrow E}$ = 15.8 ± 0.1%; Fig. S24c and S31, ESI†). The hydrazone shows no signs of photodegradation even after ten switching cycles (Fig. S18b, ESI†). The thermal $Z \rightarrow E$ isomerization half-life ($\tau_{1/2}$) was measured to be 1710 ± 75 years (Table S1, ESI†). To explore the potential use of this alkyne containing-hydrazone as a photoswitchable tag for Raman spectroscopy we also studied the change in Raman alkyne vibrational bands as a function of photoisomerization. The alkyne vibrational band associated with the **1**-*E* isomer was measured at 2085 cm^{-1} and following isomerization to the **1**-*Z* the band shifted to 2105 cm^{-1}, representing a 20 cm^{-1} shift (Fig. S42, ESI†).

To improve the band separation between the *E*/*Z* isomers we synthesized hydrazone **2** bearing a *para*-NO_2 group on the stator phenyl group. This group is known[7] to redshift the absorption spectra and improve the band separation in such hydrazones. This modification produced the desired redshift in the **2**-*E* absorption band (λ_{max} = 378 nm; Fig. 2a). Irradiation with 340 nm light resulted in a redshift of the absorption band (λ_{max} = 392 nm) and a drastically improved PSS_{340} of 80% *Z* ($\Phi_{E\rightarrow Z}$ = 30.2 ± 2.5%; Fig. S25b and S32, ESI†). The reverse $Z \rightarrow E$ isomerization was accomplished using 442 nm light resulting with a PSS_{442} > 99% *E* and $\Phi_{Z\rightarrow E}$ = 51.7 ± 0.4% (Fig. S25c and S33, ESI†). The hydrazone is photostable, allowing for 10 cycles of photoswitching without signs of degradation (Fig. S19b, ESI†). The $\tau_{1/2}$ was measured to be 2697 ± 235 years (Table S1, ESI†). The Raman spectra of the **2** showed only a 15 cm^{-1} band shift upon photoswitching (Fig. 2b).

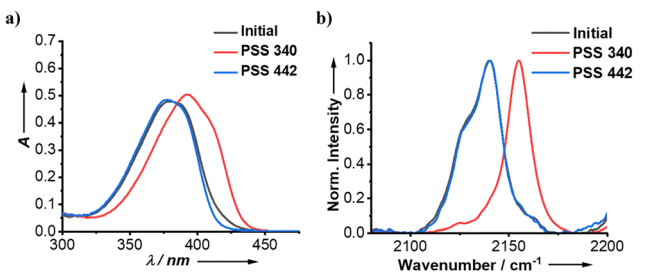

Fig. 2 (a) UV-vis spectra (initial, PSS_{340} and PSS_{442}) of **2** in toluene (1.0 × 10^{-5} M); and (b) normalized Raman spectra of the alkyne region in toluene (1.0 × 10^{-3} M).

To further investigate the effects of extending the π-conjugation in the hydrazone we synthesized **3** in which the TMS-protecting group is replaced with a phenyl moiety. As expected, this substitution resulted in an 11 nm bathochromic shift of the λ_{max} of **3**-*E* relative to **1**-*E* (Table 1 and Fig. S20a, ESI†). However, similar to **1**, hydrazone **3** also results in a significant *E*/*Z* absorption band overlap resulting in a PSS_{340} of 43% *Z* ($\Phi_{E\rightarrow Z}$ = 15.3 ± 0.6%; Fig. S26b and S34, ESI†). Irradiation of the sample with 442 nm results in excellent PSS and improved quantum yield (see Table 1 and Fig. S26c and S35, ESI†). The switch showed no signs of degradation after multiple switching cycles (Fig. S20b, ESI†), while the $\tau_{1/2}$ increased to 1929 ± 80 years (Table S1, ESI†). The Raman alkyne band shift was measured to be 21 cm^{-1} after photoswitching (Fig. S45, ESI†).

Next, and to combine the benefits of hydrazones **2** and **3** we synthesized **4**, which as expected resulted in a further redshifted *E* isomer (λ_{max} of 388 nm; Fig. S21, ESI†). Irradiation with 340 nm light resulted in a PSS_{340} of 84% *Z* (λ_{max} of 404 nm; Fig. S27b, ESI†)‡ and a comparable quantum yield (Table 1 and Fig. S36, ESI†). The $Z \rightarrow E$ isomerization with 442 nm light resulted in a PSS_{442} of 98% *E* ($\Phi_{Z\rightarrow E}$ = 47.5 ± 0.7%; Fig. S27c and S37, ESI†). Hydrazone **4** also has excellent photostability even after ten switching cycles (Fig. S21b, ESI†). The $\tau_{1/2}$ was measured at 2628 ± 123 years (Table S1, ESI†). The switch resulted in a 21 cm^{-1} change after photoswitching (Table 1 and Fig. S46, ESI†).

Finally, we studied hydrazones **5** and **6** bearing the strong electron donating *para*-NMe_2 group at the rotor, and a *para*-NO_2 group at the stator of the latter. The absorption band of the *E* isomer in both hydrazones was strongly red shifted (Table 1 and Fig. S22 and S23, ESI†). Photoswitching with 340 nm results in PSS_{340} of 57% and 75% *Z* and Φ of 11.8 ± 0.6% and 7.2 ± 0.2%, respectively (Fig. S28b, S29b, S38 and S40, ESI†). The $Z \rightarrow E$

Table 1 Summary of the photophysical properties of hydrazones **1–6**

Compound	λ_{abs}, *E* (nm)	$E:Z_{PSS}$ (%)	$E:Z_{PSS340}$(%)	$\Phi_{Z\rightarrow E}$ (%)	$\Phi_{E\rightarrow Z}$ (%)	$\tau_{1/2}$ (*y*)[d]	Raman shift (cm^{-1})
1	359	99 : 1[a]	53 : 47	15.8 ± 0.1	8.4 ± 1.1	1710 ± 75	20
2	378	99 : 1[b]	20 : 80	51.7 ± 0.4	30.2 ± 2.5	2697 ± 235	15
3	370	99 : 1[b]	57 : 43	44.9 ± 3.3	15.3 ± 0.6	1929 ± 80	21
4	388	98 : 2[b]	16 : 84	47.5 ± 0.7	17.9 ± 0.4	2628 ± 123	20
5	391	99 : 1[b]	43 : 57	34.2 ± 0.8	11.8 ± 0.6	517 ± 13	34
6	420	87 : 13[c]	25 : 75	30.1 ± 0.3	7.2 ± 0.2	392 ± 45	32

[a] PSS was achieved with 410 nm light. [b] PSS was achieved with 442 nm light. [c] PSS was achieved with 480 nm light. [d] Half-life at 298 K

isomerization process results in a PSS_{442} of >99% *E* for **5** and PSS_{480} 87% *E* for **6** ($\Phi_{Z\rightarrow E}$ = 34.2 ± 0.8% and $\Phi_{Z\rightarrow E}$ = 30.1 ± 0.3% respectively; Fig. S28c, S29c, S39 and S41, ESI†).§ Both **5** and **6** exibit signs of photodegradation consistent with behavior observed for NMe_2-substituted hydrazones[16] (Fig. S22b and S23b, ESI†). Both hydrazones also retain bistability with $\tau_{1/2}$ of 517 ± 13 and 392 ± 45 years, for **5** and **6** respectively (Table S1, ESI†). Most notably these systems show improvement in the alkyne vibrational band separation (34 cm^{-1} and 32 cm^{-1} for **5** and **6** respectively) (Fig. S47 and S48, ESI†). We hypothesize that the NMe_2 group, which enhances the conjugation in these switches, especially in the H-bonded *Z* form, is responsible for this large shift. To our knowledge, these values represent the highest recorded Raman signal shifts observed in a photoswitchable system.[15]

In conclusion, we developed a family of six easily accessible alkyne-containing hydrazones photoswitches. We found that photoswitches **1**,**3** and **5** generally suffer from overlap in the absorption bands resulting in lower PSS values. While the presence of *para*-NO_2 group at the stator, in **2**, **4** and **6**, improves the band separation, thereby improving their PSSs. Moreover, photoswitch **5** benefits greatly from the strong electron donating group, exhibiting red-shifted absorption bands without compromising bistability. Our study also demonstrates the viability of using hydrazone switching as a mechanism for changing the vibrational frequency of the alkyne group, thus making these systems viable bioimaging probes for Raman scattering spectroscopy. Specifically, switches **5** and **6** demonstrate dramatic Raman signal shift between their two isomers (>30 cm^{-1}). The resulting hydrazones enhance the structural landscape of photoswitchable alkynes that can be used in bioimaging.

The authors acknowledge the ACS PRF (66249-ND4) for the generous support.

Data availability

The data supporting this article have been included in the ESI.†

Conflicts of interest

There are no conflicts to declare.

Notes and references

‡ Intermediate irradiation wavelengths were tested, but they resulted in worse PSS values compared to those obtained with 340 nm light (Fig. S27, ESI†).

§ Irradiating **5** with other wavelengths resulted in worse PSS values (Fig. S28, ESI†), as observed for **4**. Additionally, **6** was found to be extremely unstable, preventing in-depth analysis.

1 A. Goulet-Hanssens, F. Eisenreich and S. Hecht, *Adv. Mater.*, 2020, **32**, 1905966.
2 R. Dorel and B. L. Feringa, *Chem. Commun.*, 2019, **55**, 6477–6486.
3 M. Olesińska-Mönch and C. Deo, *Chem. Commun.*, 2023, **59**, 660–669.
4 (*a*) M. M. Russew and S. Hecht, *Adv. Mater.*, 2010, **22**, 3348–3360; (*b*) C. L. Sun, C. Wang and R. Boulatov, *ChemPhotoChem*, 2019, **3**, 268–283; (*c*) Q. Qiu, Q. Qi, J. Usuba, H. Fu, I. Aprahamian and G. G. D. Han, *Chem. Sci.*, 2023, **14**, 11359–11364.
5 (*a*) B. L. Feringa, *Molecular Switches*, Wiley-VCH, 2001; (*b*) M. Irie, T. Fukaminato, K. Matsuda and S. Kobatake, *Chem. Rev.*, 2014, **114**, 12174–12277; (*c*) C. Petermayer and H. Dube, *Acc. Chem. Res.*, 2018, **51**, 1153–1163; (*d*) M. Clerc, S. Sandlass, O. Rifaie-Graham, J. A. Peterson, N. Bruns, J. Read de Alaniz and L. F. Boesel, *Chem. Soc. Rev.*, 2023, **52**, 8245–8294.
6 (*a*) X. Su, T. Lessing and I. Aprahamian, *Beilstein J. Org. Chem.*, 2012, **8**, 872–876; (*b*) X. Su, M. Lokov, A. Kutt, I. Leito and I. Aprahamian, *Chem. Commun.*, 2012, **48**, 10490–10492; (*c*) H. Qian, S. Pramanik and I. Aprahamian, *J. Am. Chem. Soc.*, 2017, **139**, 9140–9143; (*d*) L.-Q. Zheng, S. Yang, J. Lan, L. Gyr, G. Goubert, H. Qian, I. Aprahamian and R. Zenobi, *J. Am. Chem. Soc.*, 2019, **141**, 17637–17645; (*e*) B. Shao and I. Aprahamian, *Chemistry*, 2020, **6**, 2162–2173; (*f*) S. Yang, D. Larsen, M. Pellegrini, S. Meier, D. F. Mierke, S. R. Beeren and I. Aprahamian, *Chem*, 2021, **7**, 2190–2200; (*g*) S. Yang, J. D. Harris, A. Lambai, L. L. Jeliazkov, G. Mohanty, H. Zeng, A. Priimagi and I. Aprahamian, *J. Am. Chem. Soc.*, 2021, **143**, 16348–16353; (*h*) Q. Qiu, S. Yang, M. A. Gerkman, H. Fu, I. Aprahamian and G. G. D. Han, *J. Am. Chem. Soc.*, 2022, **144**, 12627–12631; (*i*) I. Bala, J. T. Plank, B. Balamut, D. Henry, A. R. Lippert and I. Aprahamian, *Nat. Chem.*, 2024, **16**, 2084–2090; (*j*) B. Shao, H. Fu and I. Aprahamian, *Science*, 2024, **385**, 544–549.
7 B. Shao, H. Qian, Q. Li and I. Aprahamian, *J. Am. Chem. Soc.*, 2019, **141**, 8364–8371.
8 D. Sosnin, M. Izadyar, S. A. A. Abedi, X. Liu and I. Aprahamian, *J. Am. Chem. Soc.*, 2025, **147**, 14930–14935.
9 (*a*) H. Yamakoshi, K. Dodo, A. Palonpon, J. Ando, K. Fujita, S. Kawata and M. Sodeoka, *J. Am. Chem. Soc.*, 2012, **134**, 20681–20689; (*b*) F. Hu, L. Shi and W. Min, *Nat. Methods*, 2019, **16**, 830–842.
10 S. Bakthavatsalam, K. Dodo and M. Sodeoka, *RSC Chem. Biol.*, 2021, **2**, 1415–1429.
11 J. X. Cheng and X. S. Xie, *Science*, 2015, **350**, 6264.
12 (*a*) L. Wei, Z. Chen, L. Shi, R. Long, A. V. Anzalone, L. Zhang, F. Hu, R. Yuste, V. W. Cornish and W. Min, *Nature*, 2017, **544**, 465–470; (*b*) F. Hu, C. Zeng, R. Long, Y. Miao, L. Wei, Q. Xu and W. Min, *Nat. Methods*, 2018, **15**, 194–200.
13 (*a*) M. Hofmann, C. Eggeling, S. Jakobs and S. W. Hell, *Proc. Natl. Acad. Sci. U. S. A.*, 2005, **102**, 17565–17569; (*b*) S. W. Hell, *Nat. Methods*, 2009, **6**, 24–32.
14 J. Shou, A. Komazawa, Y. Wachi, M. Kawatani, H. Fujioka, S. J. Spratt, T. Mizuguchi, K. Oguchi, H. Akaboshi, F. Obata, R. Tachibana, S. Yasunaga, Y. Mita, Y. Misawa, R. Kojima, Y. Urano, M. Kamiya and Y. Ozeki, *Sci. Adv.*, 2023, **9**, eade9118.
15 (*a*) J. Ao, X. Fang, X. Miao, J. Ling, H. Kang, S. Park, C. Wu and M. Ji, *Nat. Commun.*, 2021, **12**, 3089; (*b*) Y. Yang, X. Bai and F. Hu, *Nat. Commun.*, 2024, **15**, 2578.
16 B. Shao, M. Baroncini, H. Qian, L. Bussotti, M. Di Donato, A. Credi and I. Aprahamian, *J. Am. Chem. Soc.*, 2018, **140**, 12323–12327.